J|A|C|S
ARTICLES
Published on Web 12/06/2001

Structure Rationalization and Topology Prediction of Two-Distinct-Component Organic Crystals: The Role of Volume Fraction and Interface Topology

Zhengtao Xu, Stephen Lee,* Emil B. Lobkovsky, and Y.-H. Kiang

Contribution from the Department of Chemistry and Chemical Biology, Baker Laboratory, Cornell University, Ithaca, New York 14853-1301

Received June 25, 2001

Abstract: We consider here small-length-scale crystal structures with two clearly different molecular components (e.g., hydrophobic and hydrophilic). Using a perspective developed by studies on large-length-scale block copolymers and liquid crystals, we focus on the crystalline interface between the two components. We examine four types of two-component crystals: aromatic ammonium carboxylates, aromatic oligo(ethylene oxides), cyclohexylammonium carboxylates, and ether−thioether compounds. Of the 111 crystal structures found in the Cambridge Structure Database (CSD), 108 adopt one of the five generic topologies found in diblock copolymers: spheres, columns, perforated layers, layers, and bicontinuous structures. As in diblock copolymers, a key factor controlling the interfacial topology is shown to be the volume ratio of the two components. When the volume fraction of one component is less than 30% of the whole, more than five-sixths of the examined crystal structures are of columnar or spherical type. For volume fractions between 40 and 50% more than three-quarters are of lamellar or bicontinuous type. We use this model to predict the topologies of small-length-scale two-component crystals. We predict the crystal topolgies of six new crystal structures: three are predicted to be columnar, and the other three, lamellar or bicontinuous. The crystal structures of these systems were then determined by single-crystal X-ray methods. Five of the structures form in topologies consistent with the predictions: three in columns and two in layers. The remaining one forms as a perforated layer instead of the predicted columnar structure. Such predictive accuracy is consistent with the statistics of the CSD investigation.

Introduction

There has recently been a renewed interest in controlling the crystalline structures of organic-based solid-state materials.[1−44] This effort has been driven, in part, by the physical properties of such materials, properties which include porosity[45−72] potentially useful in separation, catalysis and sensing, magnetism,[73−77]electronic[32,77−83] and optical properties,[84−88] and even moderately high T_c superconductivity,[89−91] and in part by the promise of accessing the full panoply of organic molecular synthesis in the optimization of these aforementioned properties. One of the chief impediments in this undertaking is that the actual physical properties depend to a great extent not just on the molecular shape but the global crystal structure and that it is in general difficult to envision the global crystal structure from a knowledge of the shape and stoichiometry of the molecular building blocks alone.

The development of methods for relating organic molecular shapes to organic crystal structure is therefore important and is actively being pursued. By far, the most common approach is one based on building up (or Aufbau). In this viewpoint, one takes the molecular stoichiometry and structure as a given, and from this molecular data one then deduces the local bonding interactions which govern packing and thence the final crystal structure. The use of the Cambridge Structure Database (CSD) to determine common local motifs,[92−94] the idea of supramolecular chemistry in general where one concentrates on intermolecular interactions,[95−100] and the use of theoretical methods to derive crystal structures from their molecular constituents

* To whom correspondence should be addressed. E-mail: sl137@cornell.edu.

(1) Konnert, J.; Britton, D. *Inorg. Chem.* **1966**, *5*, 1193.
(2) Simard, M.; Su, D.; Wuest, J. D. *J. Am. Chem. Soc.* **1991**, *113*, 4696.
(3) Abrahams, B. F.; Hoskins, B. F.; Lin, J.; Robson, R. *J. Am. Chem. Soc.* **1991**, *113*, 3045.
(4) Ermer, O.; Lindenberg, L. *Helv. Chim. Acta* **1991**, *74*, 825.
(5) Venkataraman, D.; Lee, S.; Zhang, S.; Moore, J. S. *Nature* **1994**, *371*, 591.
(6) Ung, A.; Gizachew, D.; Bishop, R.; Scudder, M.; Dance, I.; Craig, D. *J. Am. Chem. Soc.* **1995**, *117*, 8475.
(7) Lu, J.; Harrison, W. T. A.; Jacobson, A. J. *Angew. Chem., Int. Ed. Engl.* **1995**, *34*, 2557.
(8) Endo, K.; Sawaki, T.; Koyanagi, M.; Kobayashi, K.; Masuda, H.; Aoyama, Y. *J. Am. Chem. Soc.* **1995**, *117*, 8341.
(9) Yaghi, O. M.; Li, G.; Li, H. *Nature* **1995**, *378*, 703.
(10) Dolbeq, A.; Boubekeur, K.; Batail, P.; Canadell, E.; Aubansenzier, P.; Coulon, C.; Lerstrup, K. *Mater. Chem.* **1995**, *5*, 1707.
(11) Gardner, G. B.; Venkataraman, D.; Moore, J. S.; Lee, S. *Nature* **1995**, *374*, 792.
(12) Carlucci, L.; Ciani, G.; Proserpio, D.; Sironi, A. *Chem. Commun.* **1996**, 1393.
(13) Vaid, T. P.; Lobkovsky, E. B.; Wolczanski, P. T. *J. Am. Chem. Soc.* **1997**, *119*, 8742.
(14) MacGillivray, L.; Atwood, J. *Nature* **1997**, *389*, 496.
(15) Aakeröy, C. B.; Beatty, A. M.; Leinen, D. S. *J. Am. Chem. Soc.* **1998**, *120*, 7383.
(16) Kobayashi, K.; Koyanagi, M.; Endo, K.; Masuda, H.; Aoyama, Y. *Chem. Eur. J.* **1998**, *4*, 417.
(17) Bailey, R. D.; Hook, L. L.; Pennington, W. T. *Chem. Commun.* **1998**, 1181.
(18) Batten, S. R.; Robson, R. *Angew. Chem., Int. Ed.* **1998**, *37*, 1461.

either by ab initio quantum mechanical methods or empirically derived atom−atom potentials[101−107] all belong to this category of research.

Much less traveled is the opposite approach where one looks at the outset at the final crystal topology and then derives the molecular pieces needed to coexist within such a crystalline structure. Such an approach is particularly difficult for chemists, as our concern naturally gravitates to the chemical bond, which even in the case of an ionic bonding is primarily local. A few examples of this latter approach can be found in the literature, for example the work of Robson, co-workers and others.[108−112] These authors have postulated that certain extended net topologies are generally more stable than others, topologies such as the diamond net, rutile, and PtS, and they have shown that rigid, highly symmetrical molecules and ions can be chosen to form into these same structure types.

In a recent paper[113] we proposed an alternate method of crystal design based on this crystal-to-molecule approach. In particular, we considered molecules which contain two components (e.g., hydrophobic and hydrophilic fractions). Using a perspective developed by the block copolymer and liquid crystal communities,[114−117] we focused on the long-range ordered crystalline interface between these two components. Working with aromatic oligo(ethylene oxides), we found, both in the crystal structures we prepared and those we examined in the literature, that such interfaces were generally well-defined. Over 90% of the structures examined had crystal topologies reminiscent of the five known topologies in diblock copolymers, that is, the spherical, columnar, lamellar, perforated lamellar, and bicontinuous structures. In addition, we found that a strong predictor for crystalline topology is the ratio of the volume of the hydrophobic portion to that of the overall molecule.

The following open questions remain. Can this approach be generalized, that is, do other two-component systems adopt crystal topologies such as those found for aromatic oligo(ethylene oxides)? If so, can one use this approach not just to rationalize crystal topology but also to *predict* crystal topology?

In this paper, we try to answer these questions. First, using the CSD we examined three other two-component crystal types: aromatic ammonium carboxylates where there are hydrophobic aromatic groups and hydrophilic ammonium carboxylate units, cyclohexylammonium carboxylates where now the hydrophobic portion is the aliphatic group, and finally molecules composed of thioether and ether groups where the thioether groups are considered soft and the ether moiety hard. We show that these three classes of molecules formed crystal topologies strongly reminiscent of those we had found earlier in aromatic oligo(ethylene oxides). The volume ratio of the two components is again a strong determinant of the structural topology. In two-thirds of the cases where the volume fraction of the minor portion was 20−30% of the total volume, the columnar topology is observed. In over three-quarters of the cases where the volume ratio was 40−50%, the lamellar or bicontinuous structures are observed.

In this paper we further report on the predictive accuracy of the above interfacial model. We considered six molecular systems whose crystal structures were unknown. We predicted[118] that three of these systems would form in columns while the remaining three would be either layers or bicontinuous. In this paper we use the actual crystal structures from X-ray studies to assess the accuracy of our earlier predictions.[119] In two of three cases where the column is predicted, the columnar structure was indeed found. In all three cases where a layer or bicontinuous

(19) Hagrman, P. J.; Hagrman, D.; Zubieta, J. *Angew. Chem., Int. Ed.* **1999**, *38*, 2639.
(20) Hagrman, D.; Hagrman, P. J.; Zubieta, J. *Angew. Chem., Int. Ed.* **1999**, *38*, 3165.
(21) Hagrman, P. J.; Zubieta, J. *Inorg. Chem.* **1999**, *38*, 4480.
(22) Prince, R. B.; Okada, T.; Moore, J. S. *Angew. Chem., Int. Ed.* **1999**, *38*, 233.
(23) Gong, B.; Zheng, C.; Zeng, H. Q.; Zhu, J. *J. Am. Chem. Soc.* **1999**, *121*, 9766.
(24) Gong, B.; Yan, Y. F.; Zeng, H. Q.; Skrzypczak-Jankunn, E.; Kim, Y. W.; Zhu, J.; Ickes, H. *J. Am. Chem. Soc.* **1999**, *121*, 5607.
(25) Li, H.; Eddaoudi, M.; O'Keeffe, M.; Yaghi, O. M. *Nature* **1999**, *402*, 276.
(26) Li, H.; Laine, A.; O'Keeffe, M.; Yaghi, O. M. *Science* **1999**, *283*, 1145.
(27) Kiang, Y.-H.; Gardner, G. B.; Lee, S.; Xu, Z.; Lobkovsky, E. *J. Am. Chem. Soc.* **1999**, *121*, 8204.
(28) Dong, Y. B.; Layland, R. C.; Pschirer, N. G.; Smith, M. D.; Bunz, U. H. F.; zur Loye, H. C. *Chem. Mater.* **1999**, *11*, 1413.
(29) Tong, M. L.; Chen, X. M.; Ye, B. H.; Ji, L. N. *Angew. Chem., Int. Ed.* **1999**, *38*, 2237.
(30) Karle, I. L.; Ranganathan, D.; Kurur, S. *J. Am. Chem. Soc.* **1999**, *121*, 7156.
(31) Kitazawa, T. *Chem. Commun.* **1999**, 891.
(32) Holliday, B. J.; Farrell, J. R.; Mirkin, C. A. *J. Am. Chem. Soc.* **1999**, *121*, 6316.
(33) Munakata, M.; Wu, L. P.; Ning, G. L.; Kuroda-Sowa, T.; Maekawa, M.; Suenaga, Y.; Maeno, N. *J. Am. Chem. Soc.* **1999**, *121*, 4968.
(34) Klok, H. A.; Jollife, K. A.; Schauer, C. L.; Prins, L. J.; Spatz, J. P.; Möller, M.; Timmerman, P.; Reinhoudt, D. N. *J. Am. Chem. Soc.* **1999**, *121*, 7154.
(35) Evans, C. C.; Sukarto, L.; Ward, M. D. *J. Am. Chem. Soc.* **1999**, *121*, 320.
(36) Vaid, T. P.; Tanski, J. M.; Pette, J. M.; Lobkovsky, E. B.; Wolczanski, P. T. *Inorg. Chem.* **1999**, *38*, 3394.
(37) Bock, H.; Lehn, J. M.; Pauls, J.; Holl, S.; Krenzel, V. *Angew. Chem., Int. Ed.* **1999**, *38*, 952.
(38) Biradha, K.; Domasevitch, K. V.; Moulton, B.; Seward, C.; Zaworotko, M. J. *Chem. Commun.* **1999**, 1327.
(39) Cotton, F. A.; Lin, C.; Murillo, C. A. *Chem. Commun.* **2001**, 11.
(40) Zaworotko, M. J. *Chem. Commun.* **2001**, 1.
(41) Hong, M.; Zhao, Y.; Su, W.; Cao, R.; Fujita, M.; Zhou, Z.; Chan, A. S. C. *Angew. Chem., Int. Ed.* **2000**, *39*, 2468.
(42) Min, K. S.; Suh, M. P. *Chem. Eur. J.* **2001**, *7*, 303.
(43) Sada, K.; Sugahara, M.; Kato, K.; Miyata, M. *J. Am. Chem. Soc.* **2001**, *123*, 4386.
(44) Lee, E.; Kim, J.; Heo, J.; Whang, D.; Kim, K. *Angew. Chem., Int. Ed.* **2001**, *40*, 399.
(45) Fujita, M.; Kwon, Y. J.; Washizu, S.; Ogura, K. *J. Am. Chem. Soc.* **1994**, *116*, 1151.
(46) Choe, W.; Kiang, Y.-H.; Xu, Z.; Lee, S. *Chem. Mater.* **1999**, *11*, 1776.
(47) Venkataraman, D.; Gardner, G. B.; Lee, S.; Moore, J. S. *J. Am. Chem. Soc.* **1995**, *117*, 11600.
(48) Sevov, S. C. *Angew. Chem., Int. Ed. Engl.* **1996**, *35*, 2630.
(49) Lohse, D. L.; Sevov, S. C. *Angew. Chem., Int. Ed. Engl.* **1997**, *36*, 1619.
(50) Ekambaram, S.; Sevov, S. C. *Angew. Chem., Int. Ed.* **1999**, *38*, 372.
(51) Yang, G. Y.; Sevov, S. C. *J. Am. Chem. Soc.* **1999**, *121*, 8389.
(52) Holland, B. T.; Isbester, P. K.; Blanford, C. F.; Munson, E. J.; Stein, A. *J. Am. Chem. Soc.* **1997**, *119*, 6796.
(53) Fujita, M.; Aoyagi, M.; Ogura, K. *Bull. Chem. Soc. Jpn.* **1998**, *71*, 1799.
(54) Holland, B. T.; Blanford, C. F.; Stein, A. *Science* **1998**, *281*, 538.
(55) Ranford, J. D.; Vittal, J. J.; Wu, D. *Angew. Chem., Int. Ed.* **1998**, *37*, 1114.
(56) Biradha, K.; Dennis, D.; MacKinnon, V. A.; Sharma, C. V. K.; Zaworotko, M. J. *J. Am. Chem. Soc.* **1998**, *120*, 11894.
(57) Bielawski, C.; Chen, Y. S.; Zhang, P.; Prest, P. J.; Moore, J. S. *Chem. Commun.* **1998**, 1313.
(58) Aakeröy, C. B.; Beatty, A. M.; Leinen, D. S. *Angew. Chem., Int. Ed.* **1999**, *38*, 1815.
(59) MacLachlan, M. J.; Coombs, N.; Ozin, G. A. *Nature* **1999**, *397*, 681.
(60) Soldatov, D. V.; Ripmeester, J. A.; Shergina, S. I.; Sokolov, I. E.; Zanina, A. S.; Gromilov, S. A.; Dyadin, Y. A. *J. Am. Chem. Soc.* **1999**, *121*, 4179.
(61) Holland, B. T.; Abrams, L.; Stein, A. *J. Am. Chem. Soc.* **1999**, *121*, 4308.
(62) Chui, S.; Lo, S.; Charmant, J.; Orpen, A. G.; Williams, I. D. *Science* **1999**, *283*, 1148.
(63) Gudbjartson, H.; Biradha, K.; Poirier, K. M.; Zaworotko, M. J. *J. Am. Chem. Soc.* **1999**, *121*, 2599.
(64) Khan, M. I.; Yohannes, E.; Powell, D. *Inorg. Chem.* **1999**, *38*, 212.
(65) Zaworotko, M. J. *Angew. Chem., Int. Ed. Engl.* **2000**, *39*, 3052.
(66) Noro, S.; Kitagawa, S.; Kondo, M.; Seki, K. *Angew. Chem., Int. Ed.* **2000**, *39*, 2082.
(67) Ma, B. Q.; Zhang, D. S.; Gao, S.; Jin, T. Z.; Yan, C. H.; Xu, G. X. *Angew. Chem., Int. Ed.* **2000**, *39*, 3644.
(68) Chen, B.; Eddaoudi, M.; Reineke, T. M.; Kampf, J. W.; O'Keeffe, M.; Yaghi, O. M. *J. Am. Chem. Soc.* **2000**, *122*, 11559.
(69) Zhu, J.; Bu, X.; Feng, P.; Stucky, G. D. *J. Am. Chem. Soc.* **2000**, *122*, 11563.
(70) Zheng, L. M.; Whitfield, T.; Wang, X.; Jacobson, A. J. *Angew. Chem., Int. Ed.* **2000**, *39*, 4528.

structure is predicted, the layer structure was found. These results are compatible with the statistics based on the CSD.

Experimental Section

General Procedure. Unless otherwise indicated, all commercially available reagents were purchased from Aldrich and used without further purification. Analytical grade solvents were obtained from commercial suppliers (Aldrich, Fisher Scientific, and Mallinckrodt). Powder X-ray diffraction data were recorded on an INEL MPD diffractometer (XRG 3000, CPS 120 detector) at 25 mA and 35 KV for Cu Kα1; $\lambda = 1.54056$ Å, with a silver behenate and elemental silicon standard. Lattice constants were fitted to powder data by a least-squares method. Electrospray ionization mass spectra were collected on a Micromass QUATTRO spectrometer. ^{1}H NMR and ^{13}C NMR were performed on a Bruker AF-300 spectrometer at 25 °C.

Single-crystal X-ray data were collected on a Bruker SMART diffractometer equipped with a CCD area detector using Mo Kα radiation. Single-crystal diffraction data were collected at 173 K. All structure solutions were obtained by direct method and refined using full-matrix least-squares with SHELXL 97. Tables of bond distances, bond angles, anisotropic thermal factors, observed and calculated structure factors, and powder data appear in the Supporting Information. Hydrophobic and hydrophilic cell volume and molecular closest contacts were calculated using the Cerius^2 suite of programs from MSI.[120]

1,4-Bis(β-D-glucopyranosyl)benzene (2c). 1,4-Bis(2,3,4,6-tetra-*O*-acetyl-β-D-glucopyranosyl)benzene (synthesized from known procedure[121]) (0.50 g, 1.15 mmol) was dissolved in anhydrous methanol (30 mL) in a Schlenk tube, to which a sodium hydride sample (10 mg, 0.25 mmol, 60% dispersion in mineral oil) was then added. After the hydrogen bubbles stopped forming, the tube was sealed with a septum, and the reaction mixture was stirred at room temperature for 24 h. Acidic ion-exchange resin (Dowex 50WX4-400) was then added to neutralize the base. The resin was then filtered out and the filtrate evaporated on a rotary evaporator. The resultant viscous liquid was mixed with ethyl acetate (20 mL), upon which the liquid solidified into white solid. After the ethyl acetate was decanted, methanol (30 mL) was added to recrystallize the product (0.25 g, yield 90%, white solid). ^{1}H NMR (300 MHz, 20:1 DMSO-d_6/D$_2$O) δ 6.93 (s, 4H, Ar−H), 4.69 (d, $J = 7.5$ Hz, 2H, H-1), 3.42 (dd, 2H, H-2), 3.28−3.07 (m, 10H, H-3,4,5,6); ^{13}C NMR (300 MHz, 20:1 DMSO-d_6/D$_2$O) δ 152.3, 117.2, 101.1, 76.7, 76.2, 73.0, 69.6, 60.5. ESMS (acetonitrile) *m*/*z* 452 $(M + NH_4)^+$.

X-ray Quality Single Crystal of 1,4-Bis(β-D-glucopyranosyl)-benzene (2c). 2c (1.0 mg) was dissolved in *N*,*N*-dimethylformamide (DMF) (50 mg), and the solution was placed in a glass tube (5.0 mm diameter). Acetonitrile (500 mg) was then added to the tube and swiftly mixed with the DMF solution. The tube was then covered by laboratory film (Parafilm) and left on the benchtop undisturbed. Needlelike crystals suitable for single-crystal X-ray analysis formed within 2−3 h. X-ray powder diffraction of the bulk sample showed only one crystal phase which corresponds to the single-crystal structure (see Supporting Information).

X-ray Quality Single Crystal of Dicholine Terephthalate (1a). Terephthalic acid (0.082 g, 0.49 mmol) and a choline hydroxide−water mixture (50 wt %, 0.24 g, 0.98 mmol) were dissolved in ethanol (30 mL) and stirred for 5 min. The solution was then evaporated on a rotary evaporator. The resultant viscous liquid was transferred to a Schlenk tube and evacuated on a vacuum manifold for 2 h at 90 °C. The liquid solidified in this process. Anhydrous tetrahydrofuran (THF) (20 mL) was then introduced into the Schlenk tube which was subsequently sealed by a septum and heated to 90 °C for 1 h. A small portion (about 2%) of the solid was thus dissolved. The tube was allowed to cool to 50 °C, and the mixture was filtered in nitrogen atmosphere. The filtrate was left on the benchtop sealed in a Schlenk tube with nitrogen protection. Blocklike, X-ray quality single crystals formed in the course of one week. X-ray powder diffraction of the bulk sample (precipitated from THF) showed only one crystal phase which corresponds to the single-crystal structure. (see Supporting Information).

X-ray Quality Single Crystal of Choline 2-Naphthoate (1c). The same method was applied as that for **1a**. The corresponding reagents

(71) Diskin-Posner, Y.; Dahal, S.; Goldberg, I. *Angew. Chem., Int. Ed.* **2000**, *39*, 1288.
(72) Xu, Z.; Lee, S.; Kiang, Y.-H.; Mallik, A. B.; Tsomaia, N.; Mueller, K. T. *Adv. Mater.* **2001**, *13*, 637.
(73) Karasawa, S.; Sano, Y.; Akita, T.; Koga, N.; Itoh, T.; Iwamura, H.; Rabu, P.; Drillon, M. *J. Am. Chem. Soc.* **1998**, *120*, 10080.
(74) Kaul, B. B.; Durfee, W. S.; Yee, G. T. *J. Am. Chem. Soc.* **1999**, *121*, 6862.
(75) Monfort, M.; Resino, I.; Ribas, J.; Stoeckli-Evans, H. *Angew. Chem., Int. Ed.* **2000**, *39*, 191.
(76) Miyasaka, H.; Clérac, R.; Campos-Fernández, C. S.; Dunbar, K. R. *Inorg. Chem.* **2001**, *40*, 1663.
(77) Coronado, E.; Galán-Mascarós, J. R.; Gómez-García, C. J.; Laukhin, V. *Nature* **2000**, *408*, 447.
(78) Mitzi, D. B.; Feild, C. A.; Harrison, W. T. A.; Guloy, A. M. *Nature* **1994**, *369*, 467.
(79) Mitzi, D. B.; Wang, S.; Feild, C. A.; Chess, C. A.; Guloy, A. M. *Science* **1995**, *267*, 1473.
(80) Tang, Z.; Guloy, A. M. *J. Am. Chem. Soc.* **1999**, *121*, 452.
(81) Su, W.; Hong, M.; Weng, J.; Cao, R.; Lu, S. *Angew. Chem., Int. Ed.* **2000**, *39*, 2911.
(82) Tanaka, H.; Okano, Y.; Kobayashi, H.; Suzuki, W.; Kobayashi, A. *Science* **2001**, *291*, 285.
(83) Schön, J. H.; Kloc, C.; Batlogg, B. *Nature* **2000**, *408*, 549.
(84) Zhang, H.; Wang, X.; Teo, B. K. *J. Am. Chem. Soc.* **1996**, *118*, 11813.
(85) Jiang, H.; Kakkar, A. K. *J. Am. Chem. Soc.* **1999**, *121*, 3657.
(86) Lin, W.; Wang, Z.; Ma, L. *J. Am. Chem. Soc.* **1999**, *121*, 11249.
(87) Lin, W.; Ma, L.; Evens, O. R. *Chem. Commun.* **2000**, 2263.
(88) Bénard, S.; Yu, P.; Audière, J. P.; Rivière, E.; Clément, R.; Guilhem, J.; Tchertanov, L.; Nakatani, K. *J. Am. Chem. Soc.* **2000**, *122*, 9444.
(89) Tanigaki, K.; Ebbesen, T. W.; Saito, S.; Mizuki, J.; Tsai, J. S.; Kubo, Y.; Kuroshioma, S. *Nature* **1991**, *352*, 222.
(90) Rosseinsky, M. J.; Murphy, D. W.; Fleming, R. M.; Zhou, O. *Nature* **1993**, *364*, 425.
(91) Schön, J. H.; Kloc, C.; Batlogg, B. *Nature* **2000**, *407*, 702.
(92) Etter, M. C. *Acc. Chem. Res.* **1990**, *23*, 120.
(93) Desiraju, G. R. *Crystal Engineering: the Design of Organic Solids;* Elsevier: Amsterdam, 1989.
(94) Desiraju, G. R. *Angew. Chem., Int. Ed. Engl.* **1995**, *34*, 2311.
(95) Gavezzotti, A. *Acc. Chem. Res.* **1994**, *27*, 309.
(96) Gavezzotti, A. In *Structure Correlation*; Bürgi, H. B., Dunitz, J., Eds.; VCH: Weinheim, 1994; Vol. 2.
(97) Dunitz, J.; Bernstein, J. *Acc. Chem. Res.* **1995**, *28*, 193.
(98) D. S. Reddy, D. C. Craig, G. R. D. *J. Am. Chem. Soc.* **1996**, *118*, 4090.
(99) Dunitz, J.; Taylor, R. *Chem. Eur. J.* **1997**, *3*, 89.
(100) Braga, D.; Grepioni, F.; Desiraju, G. R. *Chem. Rev.* **1998**, *98*, 1375.
(101) Williams, D. E. *J. Chem. Phys.* **1967**, *47*, 4680.
(102) Williams, D. E. *Acta Crystallogr.* **1971**, *A27*, 452.
(103) Pertsin, A. J.; Kitaigorodsky, A. I. *The Atom-Atom Potential Method;* Springer: Berlin, 1987.
(104) Kitaigorodsky, A. I. *Molecular crystals and molecules;* Academic Press: New York, 1973; pp 161−190.
(105) Perlstein, J. *J. Am. Chem. Soc.* **1994**, *116*, 455.
(106) Mooij, W. T. M.; van Eijck, B. P.; Kroon, J. *J. Am. Chem. Soc.* **2000**, *122*, 3500.
(107) Lommerse, J. P. M.; Motherwell, W. D. S.; Ammon, H. L.; Dunitz, J. D.; Gavezzotti, A.; Hofmann, D. W. M.; Leusen, F. J. J.; Mooij, W. T. M.; Price, S. L.; Schweizer, B.; Schmidt, M. U.; van Eijck, B. P.; Verwer, P.; Williams, D. E. *Acta Crystallogr.* **2000**, *B56*, 697 and references therein.
(108) Hoskins, B. F.; Robson, R. *J. Am. Chem. Soc.* **1989**, *111*, 5962.
(109) Hoskins, B. F.; Robson, R. *J. Am. Chem. Soc.* **1990**, *112*, 1546.
(110) Abrahams, B. F.; Hoskins, B. F.; Michail, D. M.; Robson, R. *Nature* **1994**, *369*, 727.
(111) Zaworotko, M. J. *Chem. Soc. Rev* **1994**, *23*, 283.
(112) Duncan, P. C. M.; Goodname, D. M. L.; Menzer, S.; Williams, D. J. *Chem. Commun.* **1996**, 2127.
(113) Xu, Z.; Kiang, Y.-H.; Lee, S.; Lobkovsky, E.; Emmott, N. *J. Am. Chem. Soc.* **2000**, *122*, 8376.
(114) Wanka, G.; Hoffmann, H.; Ulbricht, W. *Macromolecules* **1994**, *27*, 4145.
(115) Khandpur, A. K.; Förster, S.; Bates, F. S.; Hamley, I. W.; Ryan, A. J.; Bras, W.; Almdal, K.; Mortensen, K. *Macromolecules* **1995**, *28*, 8796.
(116) Noolandi, J.; Shi, A. C.; Linse, P. *Macromolecules* **1996**, *29*, 5907.
(117) Borisch, K.; Diele, S.; Göring, P.; Müller, H.; Tschierske, C. *Liq. Crys.* **1997**, *22*, 427.
(118) Xu, Z.; Lee, S.; Lee, A. J.; Lobkovsky, E. B.; Emmott, N. *Chin. J. Struct. Chem.* **2001**. In press.
(119) As will be discussed in this paper, due to difficulties in crystal growth, the actual crystals studied differ from the ones included in ref 118. However, the differences left the volume ratios unchanged or only altered by a small percentage. The earlier predictions therefore remained intact.
(120) CERIUS^2 Chemical Simulations Software Package; Molecular Simulation Inc.: San Diego, CA, 1998.
(121) Smits, E.; Engberts, J. B. F. N.; Kellogg, R. M.; van Doren, H. A. *J. Chem. Soc., Perkin Trans. 1* **1996**, 2873.

used were as follows: 2-naphthoic acid (0.084 g, 0.49 mmol), choline−water mixture (50 wt %, 0.12 g, 0.49 mmol). Crystallization over one week yielded block-shaped single crystals suitable for X-ray dataset collection. X-ray powder diffraction of the bulk sample showed only one crystal phase which corresponds to the single-crystal structure (see Supporting Information).

X-ray Quality Single Crystal of Choline Cyclohexanepropionate (3a). Cyclohexanepropionic acid (0.38 g, 2.4 mmol) and a choline hydroxide−water mixture (50 wt %, 0.59 g, 2.4 mmol) were dissolved in ethanol (30 mL) and stirred for 5 min. The solution was then evaporated on a rotary evaporator. The resultant viscous liquid was transferred to a Schlenk tube and evacuated on a vacuum manifold for 2 h at 90 °C. The liquid solidified in this process. Anhydrous THF (20 mL) was then introduced into the Schlenk tube which was subsequently sealed by a septum and heated to 80 °C. The raw product of choline cyclohexanepropionate dissolved completely. Upon cooling to room temperature, needlelike crystals suitable for X-ray dataset collection were obtained. X-ray powder diffraction of the bulk sample (precipitated from THF) showed only one crystal phase which corresponds to the single-crystal structure (see Supporting Information).

X-ray Quality Single Crystal of Choline (±)-2-*trans*-1,2-Cyclohexanedicarboxylate (3c). Cyclohexanepropionic acid (0.50 g, 2.9 mmol) and a choline hydroxide−water mixture (50 wt %, 1.40 g, 5.8 mmol) were dissolved in ethanol (30 mL) and stirred for 5 min. The solution was then evaporated on a rotary evaporator. The resultant viscous liquid was transferred to a Schlenk tube and evacuated on a vacuum manifold for 2 h at 90 °C. The liquid solidified in this process. Anhydrous acetonitrile (20 mL) was introduced into the Schlenk tube which was subsequently sealed by a septum and heated to 80 °C for 1 h. A small portion (about 5%) of the solid was thus dissolved. The mixture was filtered in nitrogen atmosphere and the filtrate was left on the benchtop in a sealed Schlenk tube under nitrogen protection. Blocklike, X-ray quality single crystals formed within 2−3 h. X-ray powder diffraction of the bulk sample (precipitated from acetonitrile) showed only one crystal phase which corresponds to the single-crystal structure (see Supporting Information).

Results

Our work is based on ideas from the diblock copolymer literature. In this field an almost universal phase diagram has been derived.[122−124] Key variables in this phase diagram are the volume ratio of the two blocks in the polymer and the driving force of segregation between the two blocks. This latter variable is usually characterized by the parameter χN. A typical example for polystyrene−polyisoprene diblock copolymers is shown in Figure 1. At low volume ratios, spheres (*s*) of one component form inside the bulk of the other component. At slightly higher volume ratios, the spheres turn into columns (*c*), while at the volume ratio of 1:1 lamellar (*l*) structures are found. Between the columnar and lamellar regions, more complex structures appear, involving either a bicontinuous (*bi*) form or a perforated layer (*pl*) structure. Finally, at the highest volume ratios, one reverses the role of the two components, where the former minor component becomes the major component and vice versa. To distinguish these structures from the previous ones, we term these topologies inverse spheres (*is*), inverse columns (*ic*), and inverse perforated layers (*ipl*). Such distinctions, however, cannot be made for layers or bicontinuous systems, since in these latter cases the two domains are topologically equivalent.

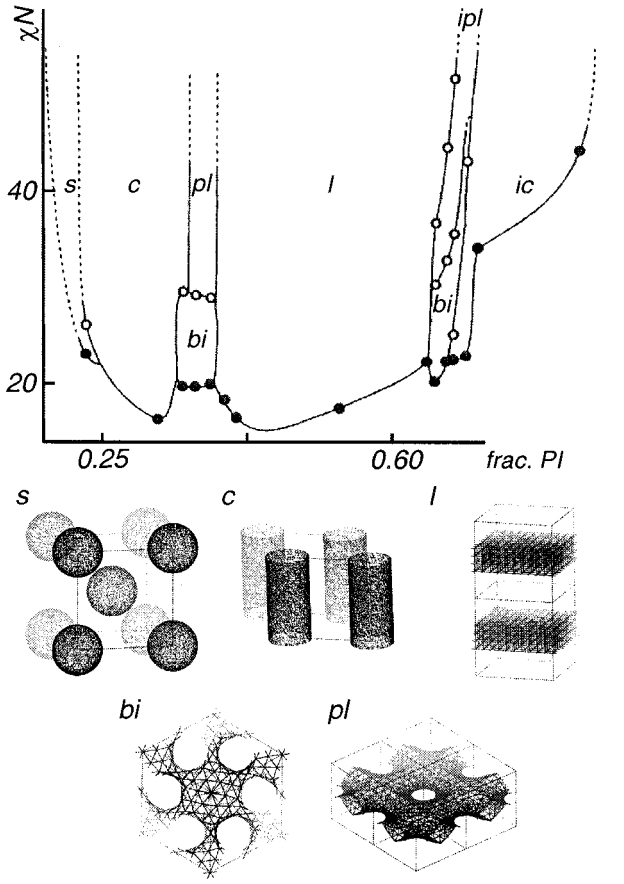

Figure 1. Experimentally determined phase diagram for PS−PI (polystyrene−polyisoprene) diblock copolymers.[115] *s*: sphere, *c*: column, *l*: layer, *bi*: bicontinuous, *pl*: perforated layer, *ipl*: inverse perforated layer, *ic*: inverse column.

The principal driving force for this structure map is the minimization of the interfacial area between the two chemical components or, alternatively, the curvature requirements of this interface. As Figure 1 shows, the volume ratio of the two components is of overarching importance.

To date very little has been done to see if this overall phase diagram is useful in the prediction and rationalization of molecular organic crystals, although significant efforts have been made to apply the concepts of minimal surfaces to solid-state crystal chemistry.[125−130] Nor at the outset is it clear that this generic framework will be useful for molecular organic crystals. The type of systems studied to date have been at nanometer scales ranging up to 1000 Å in unit cell axes.[122,131−135] At such large distances, the fluctuations caused by individual anisotropic chemical bonds will be minimized. As we approach 5−10 Å, the typical unit cell lengths of molecular crystals, even the

(122) Thomas, E. L.; Lescanec, R. L. Phase Morphology in Block Copolymer Systems. In *Self-order and Form in Polymeric Materials*; Keller, A., Warner, M., Eds.; Chapman & Hall: London, 1995; Chapter 10.
(123) Hamley, I. W. *The Physics of Block Copolymers;* Oxford University Press: New York, 1998.
(124) Diele, S.; Brand, P.; Sackmann, H. *Mol. Cryst. Liq. Cryst.* **1972**, *17*, 163.
(125) von Schnering, H. G.; Nesper, R. *Angew. Chem., Int. Ed. Engl.* **1987**, *26*, 1059.
(126) Anderson, S. *Angew. Chem., Int. Ed. Engl.* **1983**, *22*, 69.
(127) Hyde, S. T.; Anderson, S. *Z. Kristallogr.* **1986**, *174*, 225.
(128) Nesper, R. *Angew. Chem., Int. Ed. Engl.* **1991**, *30*, 789.
(129) Kiang, Y. H.; Lee, S.; Xu, Z.; Choe, W.; Gardner, G. B. *Adv. Mater.* **2000**, *12*, 767.
(130) Chen, B.; Eddaoudi, M.; Hyde, S. T.; O'Keeffe, M.; Yaghi, O. M. *Science* **2001**, *291*, 1021.
(131) Luzzati, V.; Spegt, P. A. *Nature* **1967**, *215*, 701.
(132) Hajduk, D. A.; Harper, P. E.; Gruner, S. M.; Kim, C. C. H. G.; Thomas, E. L.; Fetters, L. J. *Macromolecules* **1994**, *27*, 4063.
(133) Mogi, Y.; Nomura, M.; Kotsuji, H.; Ohnishi, K.; Matsushita, Y.; Noda, I. *Macromolecules* **1994**, *27*, 6755.
(134) Longley, W.; McIntosh, T. J. *Nature* **1983**, *303*, 612.
(135) Larsson, K. *Nature* **1983**, *304*, 664.

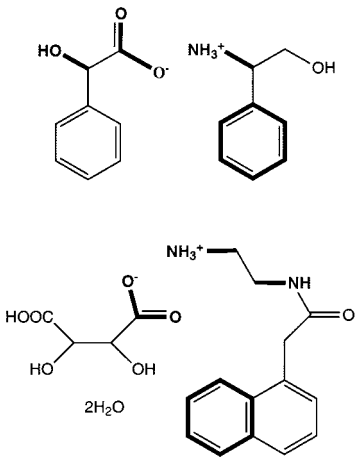

Figure 2. Representative compounds from CSD search for aromatic ammonium carboxylates. Top: *pivbax*, bottom: *ligxee*. Shown in bold are the core units: the benzenoid ring, the $C-N^+$, COO^- ion pair and the C−O or C−N bond. All nonaromatic carbon atoms are bonded to nitrogen or oxygen atoms or carbonyl groups.

concept of the interface is less well-defined. Nevertheless, as we previously noticed,[113] many molecular crystals continue to adopt structures reminiscent of those of Figure 1.

To test the usefulness of the interfacial model in molecular crystalline systems, we have retrieved from CSD four types of compounds containing two chemically distinct components. The four systems studied are aromatic ammonium carboxylates, aromatic oligo(ethylene oxides), aliphatic ammonium carboxylates, and finally molecules composed of both ether and thioether groups. In each system, in keeping with the general phase diagram of Figure 1, two distinct components are present.

Aromatic Ammonium Carboxylates. We examined the CSD for ammonium carboxylate salts. We searched for structures which contain a benzenoid ring, an ammonium carboxylate ion pair, and an additional nitrogen or oxygen atom. Such fragments are shown in the two compounds of Figure 2. We considered crystals containing only carbon, oxygen, nitrogen, and hydrogen atoms. We have excluded any structure that contains multiple-bonded nitrogen atoms. Also excluded are aliphatic carbon atoms bonded to none of the following: an oxygen atom, a nitrogen atom, or a carbonyl group. This search uncovered a total of 16 crystal structures.

We divide these ammonium carboxylate salts into their hydrophobic and hydrophilic components. The aromatic rings are hydrophobic; the oxygen and nitrogen atoms and carbonyl groups are hydrophilic. All other atoms are bonded to the above hydrophilic fragments. They are therefore considered hydrophilic. In short, the division is between the aromatic and nonaromatic groups. Furthermore, in the actual structure, the hydrophobic aromatic groups tend to aggregate with each other, and likewise the hydrophilic moieties associate with other hydrophilic moieties. As a consequence, the unit cell of the crystal structure separates into two distinct regions with a well-defined interface between them.

We now wish to classify the topologies of these different hydrophobic−hydrophilic interfaces. One expedient classification is based on interatomic distances between neighboring hydrophobic or hydrophilic groups. In particular, we define a cutoff distance: neighboring groups whose shortest interatomic distance is less than this cutoff are said to be in contact with one another. We then consider the hydrophobic groups by themselves. Hydrophobic groups which are in contact with one another can form isolated fragments, one-dimensional columns, two-dimensional sheets, or fully three-dimensional networks. In just the same way we can classify the hydrophilic portion of the crystal. We then identify if the structure belongs to the five topologies commonly observed in block copolymers. In the lamellar structure both the hydrophobic and hydrophilic portions each separately form two-dimensional sheets. In the columnar structure, one portion forms in parallel one-dimensional columns, while the other portion forms a single three-dimensional network; in spherical structures, one portion forms in isolated fragments, while the other is purely three-dimensional; in a perforated layer structure, one portion is in two-dimensional sheets, while the other is three-dimensional. Finally in the bicontinuous structure, both portions form three-dimensional networks.

While such definitions are formally rigorous, they are dependent on the definition of a contact. We base our definition of contacts on atomic van der Waals radii.[136] Even here some further thought is required. If one defines a contact as being between two atoms whose interatomic distance is less than the sum of the respective van der Waals radii, then on the whole, relatively few neighboring groups are in contact with one another, too few for any meaningful topological assignments. Conversely, if we define contacts to be between atoms whose interatomic distance is 1.5 times the sum of their respective van der Waals radii, one tends to get a great number of contacts and most networks are three-dimensional. However, for contacts defined to be 1.15−1.30 times the sum of the atomic van der Waals radii, one arrives at very reasonable structural assignments. First, as is illustrated in Figure 3, such structural assignments correspond to the overall appearance of the structure. Second, choosing the value 1.15−1.30 has little impact on the topology type: in only 15% of the cases does this range of cutoffs lead to differing assignments. Such definitions are stable.

Using the above method, we have classified the topologies of the crystal structures. Overall, we found that all 16 structures uncovered by the CSD search break down into the columnar, lamellar, and perforated lamellar types. As just mentioned, the overall classification is only slightly affected by the closest contact cutoff limit between 1.15 and 1.30. We present here the results based on a closest contact cutoff limit of 1.30. Five of the structures form into the columnar type, one has a perforated lamellar structure, and the remaining 11 belong to the lamellar family. Shown in Figure 3 are representative views of two of the columnar and four of the lamellar structures; the remainder are included in the Supporting Information.

We now study the relation between these interfacial topologies and the hydrophobic-to-total volume ratios. Specifically, we wish to see if the topologies are controlled by volume ratios in ways similar to those of block copolymers. We first need to obtain the hydrophobic-to-total volume ratio for each structure. We use atomic van der Waals radii to define atomic size. To calculate the volume ratio, we separate the crystals into the hydrophobic and hydrophilic portions (see above) and calculate the volumes for these two parts. With the volume ratios at hand, we turn to correlating the topologies with the volume ratios.

(136) Bondi, A. *J. Phys. Chem.* **1964**, *68*, 441.

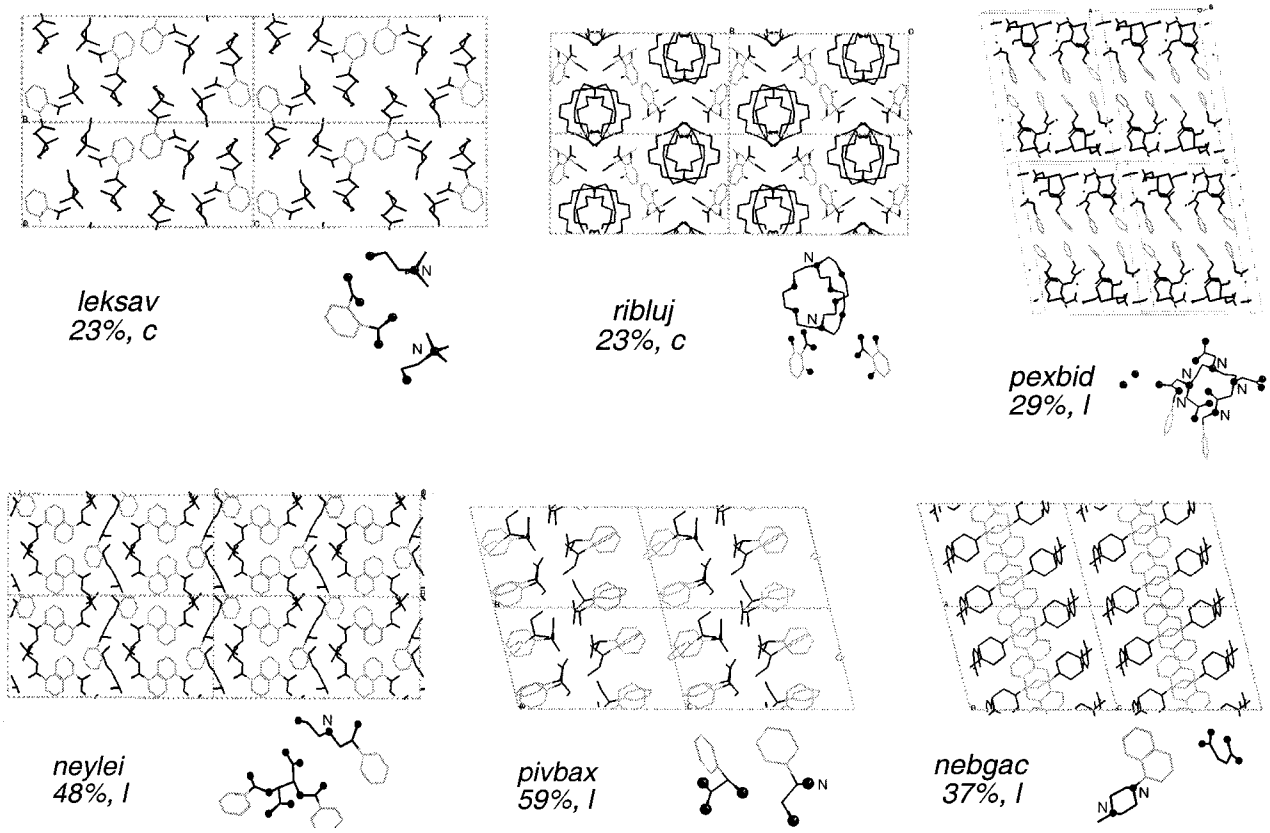

Figure 3. Structures from CSD search for aromatic ammonium carboxylates. Columns (*c*): *leksav*, *ribluj*; layers (*l*): *pexbid*, *neylei*, *pivbax*, *nebgac*. Hydrophobic portion: gray, hydrophilic portion: black. Unlabeled spheres are oxygen atoms, vertexes without spheres are carbon atoms. For clarity, hydrogen atoms are omitted. Percentages refer to the hydrophobic-to-total volume ratios.

Table 1. Structure Types and Hydrophobic-to-Hydrophilic Volume Ratios[a] in Aromatic Ammonium Carboxylates

hydrophobic-to-hydrophilic volume ratios (%)	*s*	*c*	*pl*	*l*	*ipl*	*ic*	*is*
10−20	–	–	–	–	–	–	–
20−30	–	3	–	2	–	–	–
30−40	–	–	–	3	–	–	–
40−50	–	–	1	4	–	–	–
50−60	–	–	–	3	–	–	–
60−70	–	–	–	–	–	–	–
70−80	–	–	–	–	–	–	–

[a] Structural classification is based on closest contacts defined as less than 1.30 times the sum of the van der Waals radii. *s*: sphere, *c*: column, *pl*: perforated layer, *l*: layer, *ipl*: inverse perforated layer, *ic*: inverse column, *is*: inverse sphere.

As seen in Table 1, the columnar structures are concentrated in the volume ratio region of 20−30%, whereas the lamellar structures formed predominantly in the higher region from 30−60%.

As the number of structures is rather small, based on statistics alone, we cannot at this point conclude with certainty that the hydrophobic−hydrophilic interface is a dominant structural feature. More can be learned if we look at the actual crystal structures. We consider the 11 lamellar phases. If the lamellar classification is pertinent, not only should they meet our defined criterion for lamellar structures, but the actual shape of the interface between the hydrophobic and hydrophilic portions should be well-defined. If interfacial energy is an important factor in small molecular crystal structures, we expect to see relatively smooth interfaces. In 10 out of the 11 lamellar phases, the interface is indeed smooth. In Figure 3, we portray the hydrophobic portions in gray and the hydrophilic in black. The interface is therefore between the gray and black regions. Three of these smooth interfaces (*pexbid*, *pivbax*, and *nebgac*) are shown in Figure 3, the rest are in the Supporting Information. Only in one case, that of *neylei*, also shown in Figure 3, is the interface corrugated. That most of the interfaces are smooth implies that the interfacial area tends to be minimized in the crystal structure.

Finally, we mention some additional features of these crystal structures. In terms of local structure, the aromatic rings aggregate through the typical face-to-face or face-to-edge interactions, while cationic ammonium groups in general stay close to the anionic carboxylate groups. Also of interest is the ordering of the columns in the columnar structures. Unlike in diblock copolymers where such columns are in general hexagonally ordered, in the crystal structures discussed here columnar ordering ranges from the pseudohexagonal pattern of *leksav* to a nearly rectangular array of *ribluj*, see Figure 3. We do not have sufficient crystal data to analyze the factors controlling the hexagonal versus the rectangular arrays.

Structure Topology Prediction for Aromatic Ammonium Carboxylates. The above analysis shows that one can rationalize heterogeneous crystal topologies by examining the interface between the different crystal components. Even of more interest is to use such interfaces in a *predictive* sense. We consider aromatic ammonium carboxylates.

In the above section we found that the main division was between columns and layers. In particular, columnar structures were found for volume ratios between 20% and 30%. Therefore,

for a columnar structure, we should choose a volume ratio close to 25%; to access the lamellar structure, we would prefer volume ratios around 45%.

With this in mind we examined two compounds whose crystal structures have hitherto not been determined. They are dicholine terephthalate (**1a**) and choline 2-naphthoate (**1c**). Both systems

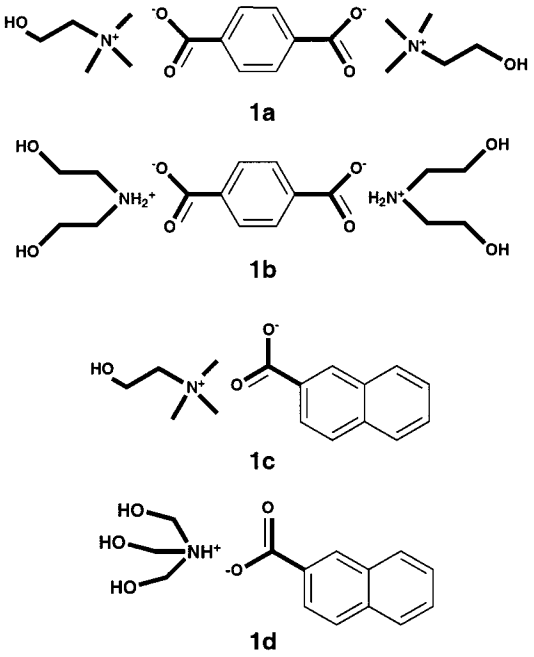

contain hydrophobic aromatic and hydrophilic ammonium carboxylate groups. The volume ratio in dicholine terephthalate is 25%; it is therefore predicted to form in the columnar type. The ratio in choline 2-naphthoate is 45%; it is predicted to be lamellar. By contrast, the shapes of the molecules are compatible with both columnar and lamellar topologies. For example, in the case of dicholine terephthalate, **1a**, although the volume ratio suggests a columnar structure, one can envision a hypothetical layer structure in which the aromatic rings lie parallel to one another, sandwiched between a hydrophilic layer composed of carboxylate groups and ammonium counterions. The determination of the actual crystal structures therefore constitutes a reasonable test as to whether we can predict interfacial topology by examining volume ratios.

In an earlier communication, we published predictions for such aromatic ammonium carboxylates.[118] The compounds reported here were synthesized after we had submitted the earlier report. It should be noted, however, that, due to the problem of obtaining single crystals, we substituted the choline group for the initially proposed groups of diethylamine and triethylamine. Thus, we report here the crystal structure of **1a** instead of **1b** and **1c** instead of **1d**. This substitution made no change in the volume ratio for **1c** and slightly shifted the volume ratio of **1a** from 26 to 21%. Thus, the actual prediction for structure topology remains unchanged.

The X-ray single-crystal structure of dicholine terephthalate is shown in Figure 4 (see also Table 2). The aromatic rings form columns running in the *a* direction. Surrounding these aromatic groups are the hydrophilic carboxylate groups and choline ions. The crystal structure clearly conforms to the earlier prediction of a columnar topology.

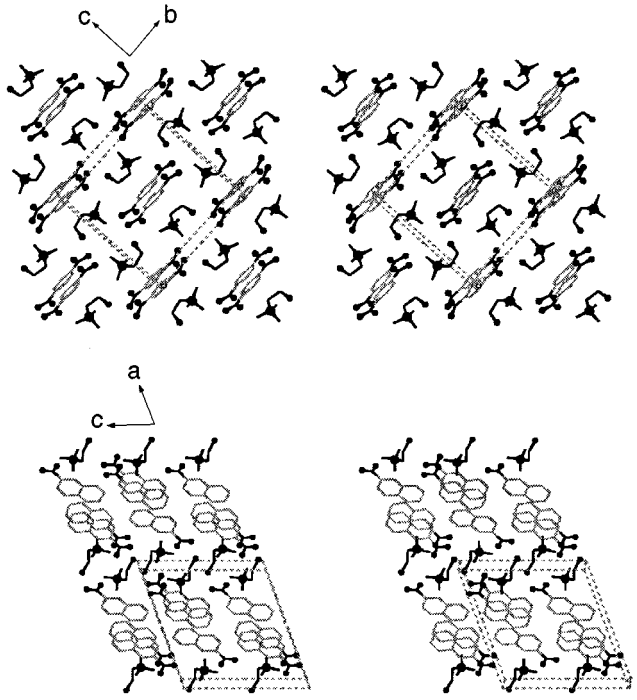

Figure 4. Crystal structures of dicholine terephthalate **1a** (top) and choline 2-naphthoate **1c** (bottom). Nitrogen atoms: large spheres, oxygen atoms: small spheres; hydrophilic portion: black, hydrophobic portion: gray. As predicted, **1a** forms in a columnar structure, **1c** a layer.

The other aspects of the structure are reasonable. The crystal forms in the space group of $P2_1/c$. The terephthalate group is located at the inversion center of the lattice, and the asymmetric unit contains one-half of this group and one choline cation. The terephthalate groups are lined up in columns with the aromatic planes parallel one to another (interplanar distance, 3.6 Å). Viewed along the column, the terephthalate moieties are surrounded by six choline groups, a common packing pattern seen in molecular crystals. Efficient packing of the molecular species is thus achieved. At the same time, such packing completes the columnar interface. As for the other interactions, the carboxylate groups stay close to the ammonium ions (closest O−N distance 3.6 Å), apparently due to electrostatic interactions. The carboxylate is also hydrogen-bonded to the hydroxyl group on the choline fragment (O−O distance 2.62 Å).

The crystal structure of choline naphthoate also conforms to the predicted topology: it is of the lamellar type, see Figure 4 and Table 2. The hydrophobic naphthalyl groups separate from the hydrophilic carboxylates and choline fragments, forming two types of lamellar domains alternating with each other. The interface between the two domains is flat as is expected of an optimized interfacial interaction.

The space group of the crystal is again $P2_1/c$. The unit cell contains four crystallographically equivalent choline−naphthoate ion pairs. The planar naphthoate fragment stacks to form the above-mentioned layers parallel to the *bc* plane. The aromatic rings therein are associated through face-to-edge interactions (closest C−C distance 3.8 Å) as well as face-to-face interactions (interplanar distance 3.6 Å). The carboxylate groups sit on both sides of the aromatic layer and form part of the hydrophilic layer. As in dicholine terephthalate, the carboxylate group is close to the ammonium cation (O−N distance 3.8 Å). It also forms a hydrogen bond with the hydroxyl portion of the choline group (O−O distance 2.6 Å).

Table 2. Crystal Data and Structure Refinements for Compounds **1a**−**3c**

	1a	1c	2c	3a	3c
formula	$C_{18}H_{32}N_2O_6$	$C_{16}H_{21}NO_3$	$C_{18}H_{28}O_{13}$	$C_{14}H_{29}NO_3$	$C_{18}H_{38}N_2O_6$
mol wt	372.46	275.34	452.40	259.38	378.50
T (K)	173(2)	173(2)	173(2)	173(2)	173(2)
wavelength (Å)	0.71073	0.71073	0.71073	0.71073	0.71073
system	monoclinic	monoclinic	monoclinic	monoclinic	monoclinic
space group	$P2_1/c$	$P2_1/c$	$P2_1$	$P2_1$	$P2_1/c$
a (Å)	6.0656(5)	14.39(1)	4.605(1)	8.830(3)	13.01(1)
b (Å)	12.173(1)	8.450(6)	23.757(4)	6.403(2)	10.22(1)
c (Å)	12.992(1)	13.259(6)	9.146(3)	13.395(7)	15.47(1)
β (deg)	91.654(2)	113.65(8)	95.037(8)	92.93(2)	102.61(5)
V (Å^3)	958.9(1)	1476(2)	996.7(4)	756.3(5)	2006(4)
Z	2	4	2	2	4
ρ_{calc} (g/cm^3)	1.290	1.239	1.507	1.139	1.253
absp coeff (mm^{-1})	0.096	0.085	0.130	0.078	0.093
θ range (deg)	3.14−30.59	2.86−23.36	2.39−23.33	2.31−23.30	1.60−20.81
limiting indices	$-8 \le h \le 8$	$-14 \le h \le 16$	$-4 \le h \le 5$	$-9 \le h \le 9$	$-13 \le h \le 13$
	$-16 \le k \le 17$	$-9 \le k \le 9$	$-19 \le k \le 26$	$-7 \le k \le 7$	$-7 \le k \le 10$
	$-18 \le l \le 16$	$-14 \le l \le 14$	$-10 \le l \le 3$	$-11 \le l \le 14$	$-15 \le l \le 14$
data/restraints/parameters	2699/0/182	2136/0/265	2564/1/288	2124/1/279	2094/0/235
measd reflns	11802	8265	3181	3996	6664
unique reflns	2699	2136	2564	2124	2094
absp correction	SADABS	SADABS	SADABS	SADABS	SADABS
GOF on F^2	1.111	0.976	0.959	0.973	1.042
R_{int}	0.0293	0.0448	0.0422	0.0561	0.0900
R1 ($I > 2\sigma(I)$)[a]	0.0539	0.0343	0.0543	0.0471	0.0699
w$R2$ ($I > 2\sigma(I)$)[b]	0.1272	0.0757	0.1067	0.0794	0.1335

[a] $R1 = \sum||F_c| - |F_o||/\sum|F_o|$. [b] $wR2 = [\sum[w((F_o^2 - F_c^2)]^2/\sum[w(F_o^2)^2]]^{1/2}$.

Table 3. Structure Types and Hydrophobic-to-Hydrophilic Volume Ratios[a] in Aromatic Oligo(ethylene oxides)

hydrophobic-to hydrophilic volume ratios (%)	*s*	*c*	*pl*	bi	*l*	*ipl*	*ic*	*is*
0−10	−	1	−	−	−	−	−	−
10−20	−	1	−	−	−	−	−	−
20−30	2	8	1	−	−	−	−	−
30−40	−	9	4	2	3	−	−	−
40−50	−	−	−	5	5	−	−	−
50−60	−	−	−	−	1	3	1	−
60−70	−	−	−	−	−	1	-	−
70−80	−	−	−	−	−	−	1	−
80−90	−	−	−	−	−	−	−	1

[a] Structural classification is based on closest contacts defined as less than 1.3 times the sum of the van der Waals radii. *s*: sphere, *c*: column, *pl*: perforated layer, *bi*: bicontinuous, *l*: layer, *ipl*: inverse perforated layer, *ic*: inverse column, *is*: inverse sphere.

Aromatic Oligo(ethylene oxides). To determine the generality of this methodology, we examined other classes of molecules containing both hydrophobic and hydrophilic portions. We turn first to aromatic oligo(ethylene oxides). Here, the hydrophobic groups are aromatic groups, the hydrophilic ones are oligo(ethylene oxides) units. As before, we focus on the topology of the interface between these two portions. Here, we briefly review a previously published CSD investigation to provide the necessary context for the predictions for specific molecules.

In our earlier search,[113] we looked for structures containing the core units of the hydrophobic benzenoid and the hydrophilic di(ethylene oxide) fragments. The search yielded 49 structures. The classification of the interfacial topology, as well as the calculation of the volume ratio was based on the methods in the above section. The interface topology showed stability similar to that of the previous set as to the definition of closest contact. Among the 49 structures, all but three were found to be of the spherical, columnar, perforated lamellar, lamellar, and bicontinuous topologies. Shown in Table 3 is the correlation between structure type and volume ratio.

We now wish to predict crystal topologies for molecules consisting of such aromatic and ethylene oxide units. Again we have chosen the columnar and the lamellar or bicontinuous topologies: a compound with a volume ratio around 25% is predicted to form the columnar type; one with 45% is predicted to be lamellar or bicontinuous. With these values in mind, we initially designed molecules **2a** and **2b**. Both molecules consist

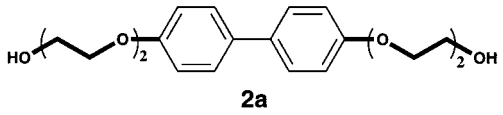

2a

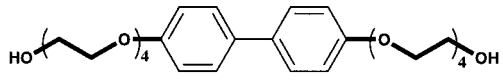

2b

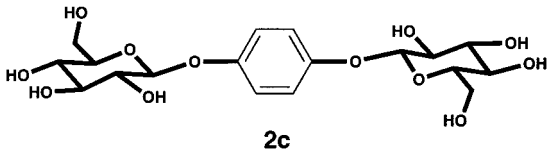

2c

of the hydrophobic aromatic groups covalently attached to hydrophilic oligo(ethylene oxide) chains. In **2a**, the molecular components give a hydrophobic-to-hydrophilic volume ratio of 45%. In our earlier work we predicted this crystal would pack in either a lamellar or bicontinuous fashion. In **2b**, as the ratio is 25%, we predicted a column. In the course of experiment, while **2a** readily yielded an X-ray quality single crystal, the crystals of **2b** turned out to be overly thin and irregular in morphology. As after repeated tries we were unable to obtain an X-ray single-crystal dataset, we examined another compound, 1,4-bis(β-D-glucopyranosyl)benzene (**2c**). It has a volume ratio of 22%, similar to that found for **2b**. The prediction for the columnar structure therefore stays the same. It should be mentioned that the volume ratio was calculated before the

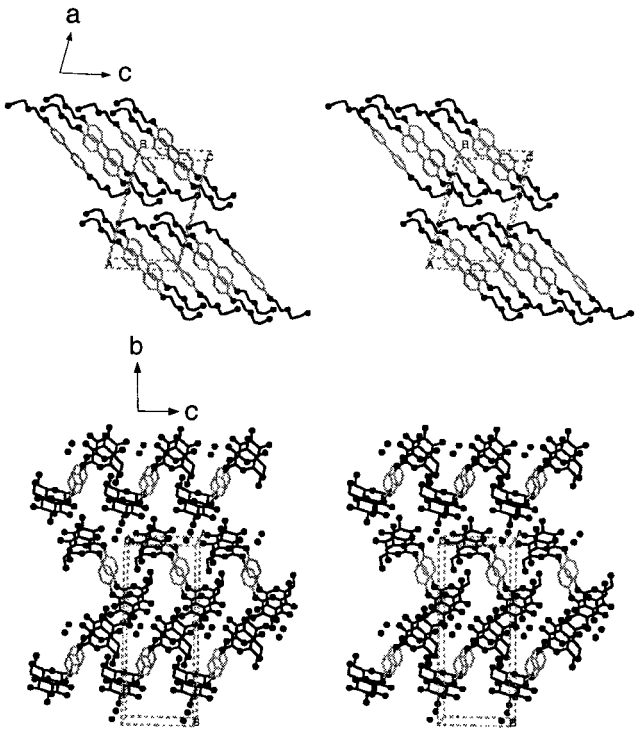

Figure 5. Crystal structures of **2a** (top) and **2c** (bottom). oxygen atoms: small spheres; hydrophilic portion: black, hydrophobic portion: gray.

synthesis of the molecule. With compound **2c** we succeeded in obtaining X-ray quality single crystals.

As previously published, the crystal structure of **2a** bears out the above prediction, forming a lamellar topology.[118] As seen at the top of Figure 5, the aromatic unit and the oligo(ethylene oxide) groups segregrate from each other, leading to distinct and regular lamellar regions. The newly solved crystal structure of **2c** (see Table 2) also conforms to our prediction. As shown at the bottom of Figure 5, the aromatic rings are stacked parallel one to another (shortest interplanar C−C distance 3.55 Å), forming columns running along the *a* axis. Surrounding the columns are the hydrophilic glucopyranosyl groups and an adventitious water molecule. The columns are arranged in a nearly hexagonal pattern. The adventitious water molecule slightly lowers the volume ratio from 22 to 20%, a value still within the columnar region.

The chiral molecules **2c** are packed into the space group $P2_1$ with two crystallographically equivalent molecules in each unit cell. Also included in the unit cell are two water molecules related by the 2_1 axis. Four hydrogen bonds are formed between each water molecule and the neighboring hydroxyl groups (O−O distances being 2.66, 2.67, 2.70, and 2.95 Å). The glucopyranosyl group adopts the usual chair conformation. Extensive hydrogen-bonding networks are formed among the hydroxyl groups. We note that although such hydrogen bonding enforces an association of the hydrophilic groups it does not distort the shape of the interface between the hydrophilic and hydrophobic groups. Down the *a* axis, one sees six nearest neighbors in the plane around each organic molecule, a common packing motif in molecular crystals.

Aliphatic Ammonium Carboxylates. We now consider a system in which the separation is between alkyl groups (hydrophobic) and groups such as ammonium carboxylates, amines, and alcohols (hydrophilic). Some caution is however needed, as it is well-known that linear alkyl chains tend to interdigitate and form layers irrespective of the actual hydrophobic-to-hydrophilic volume ratio (we comment on this later). To avoid such effects, we need to exclude such alkyl chains in both the CSD study and structure prediction. Here, we have restricted the aliphatic groups to be the cyclohexyl moiety.

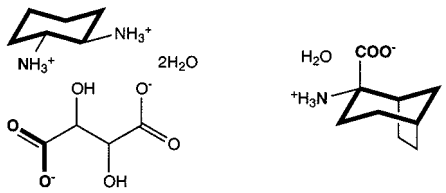

Figure 6. Representative compounds from CSD search for cyclohexylammonium carboxylates. Left: *zaνyaw*, right: *abcocx*. Shown in bold are the core units: the cyclohexyl group, the carboxylate group, and the nitrogen atom.

Table 4. Structure Types and Hydrophobic-to-Hydrophilic Volume Ratios[a] in Cyclohexyl Ammonium Carboxylates

hydrophobic-to-hydrophilic volume ratios (%)	*s*	*c*	*pl*	bi	*l*	*ipl*	*ic*	*is*
10−20	–	–	–	–	–	–	–	–
20−30	1	2	–	–	–	–	–	–
30−40	–	–	–	1	1	–	–	–
40−50	–	–	1	–	1	–	–	–
50−60	–	–	–	–	4	1	–	–
60−70	–	–	–	–	–	–	1	–
70−80	–	–	–	–	–	–	–	–

[a] Structural classification is based on closest contacts defined as less than 1.15 times the sum of the van der Waals radii.

In the CSD search, we required the essential fragments to be: a hexagon of sp^3 carbon atoms, a carboxylate group and a nitrogen atom. We considered crystals containing only carbon, hydrogen, oxygen, and nitrogen atoms. We excluded multiple bonds between carbon atoms and further required that the alkyl portion of the crystal be a continuous fragment (i.e., not split by the hydrophilic groups). Such a search yielded 15 structures, most of which are nonnatural amino acids containing the cyclohexyl group. Figure 6 shows two representative compounds.

The oxygen and nitrogen atoms and carbon atoms bonded to them are considered hydrophilic. The remaining atoms constitute the alkyl portion and are hydrophobic. On the basis of the closest contacts mentioned earlier, 13 of the 15 structures were classified into the five generic topologies. For the two remaining structures, while at the cutoff limit of 1.30, they are respectively of layer (*zaνxup*) and bicontinuous topology (*ammchc10*), at a cutoff of 1.15; however, their topologies change. In *ammchc10* both the hydrophilic and hydrophobic parts become one-dimensional; in *zaνxup*, the hydrophobic portion becomes one-dimensional while the hydrophilic portion remains two-dimensional. Between the cutoff limits of 1.30 and 1.15, two other structures switch their classifications, one from layer to column and another from inverse perforated layer to inverse column. As Tables 4 shows, for a cutoff of 1.15 one finds a correlation between volume ratios and crystal topology statistically compatible with the phase diagram of Figure 1, and those of Tables 2 and 3. The correlation for a cutoff of 1.30 becomes slightly less good, see Table 5.

Shown in Figure 7 are six of the layer structures reported in

Table 5. Structure Types and Hydrophobic-to-Hydrophilic Volume Ratios[a] in Cyclohexyl Ammonium Carboxylates

hydrophobic-to-hydrophilic volume ratios (%)	*s*	*c*	*pl*	*pl*	*l*	*ipl*	*ic*	*is*
10−20	−	−	−	−	−	−	−	−
20−30	1	1	−	−	2	−	−	−
30−40	−	−	−	1	1	−	−	−
40−50	−	−	1	−	1	−	−	−
50−60	−	−	−	1	4	1	−	−
60−70	−	−	−	−	−	1	−	−
70−80	−	−	−	−	−	−	−	−

[a] Structural classification is based on closest contacts defined as less than 1.3 times the sum of the van der Waals radii. *s*: sphere, *c*: column, *pl*: perforated layer, *bi*: bicontinuous, *l*: layer, *ipl*: inverse perforated layer, *ic*: inverse column, *is*: inverse sphere.

Table 4. As can be seen in this figure, the layer topologies are generally smooth and regular, conforming well to the interfacial model.

In predicting crystal topologies we again target the columnar and lamellar structure types. In particular, we first considered compounds **3a** and **3b**. As before, we calculate the hydrophobic−hydrophilic volume fraction from the molecular composition and thereby predict the crystal structure type. In **3a**, the hydrophobic volume fraction is 46%, and the crystal structure is predicted to be lamellar or bicontinuous; in **3b**, the volume fraction is 25%, and the structure is predicted to be columnar. Again only after reporting our predictions did we proceed to the experiments. Compound **3a** readily yielded X-ray quality crystals, but compound **3b** proved difficult even to solidify at room temperature. We therefore turned to a related compound, **3c**, which has a similar volume fraction (23%). Prior to synthesis, we predicted it to form a columnar crystal structure. Fortunately, we were able to crystallize **3c** well enough to afford an X-ray single-crystal dataset.

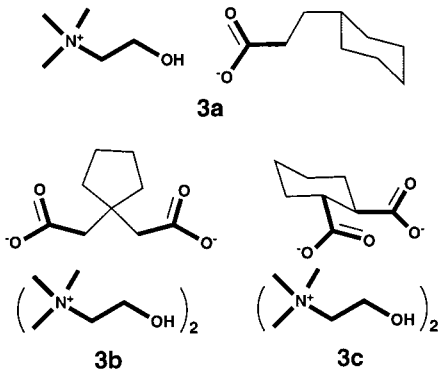

We show the crystal structure of **3a** in Figure 8. As predicted, it is of lamellar type. A clear boundary is formed between the hydrophobic cyclohexyl groups and the hydrophilic choline and carboxylate groups. The compound crystallized in the noncentrosymmetric space group of $P2_1$. The asymmetric unit of each cell consists of one cyclohexylpropionate group and one choline group. The cyclohexyl groups adopt the usual boat conformation, and the propionate groups take the equatorial position. The cyclohexyl groups are packed to form the hydrophobic layers, which are parallel to the *ab* plane. Within the layer, the cyclohexyl groups are related by the 2_1 screw axis, and each cyclohexyl group has six nearest neighboring cyclohexyl groups. The propionate groups are located on both sides of the layer. Between layers of the cyclohexyl groups are the choline units, which together with the carboxylate groups form the hydrophilic layer. The carboxylate is hydrogen-bonded to the choline unit via the OH group (O−O distance 2.61 Å).

The crystal structure of **3c** is shown in Figure 8. At a volume ratio of 23%, it was predicted to be a columnar structure. Instead the structure of **3c** proved to be of the perforated lamellar type. We recall that in our CSD analysis, within the volume ratio range of 20−30%, while columns are the major phase, other

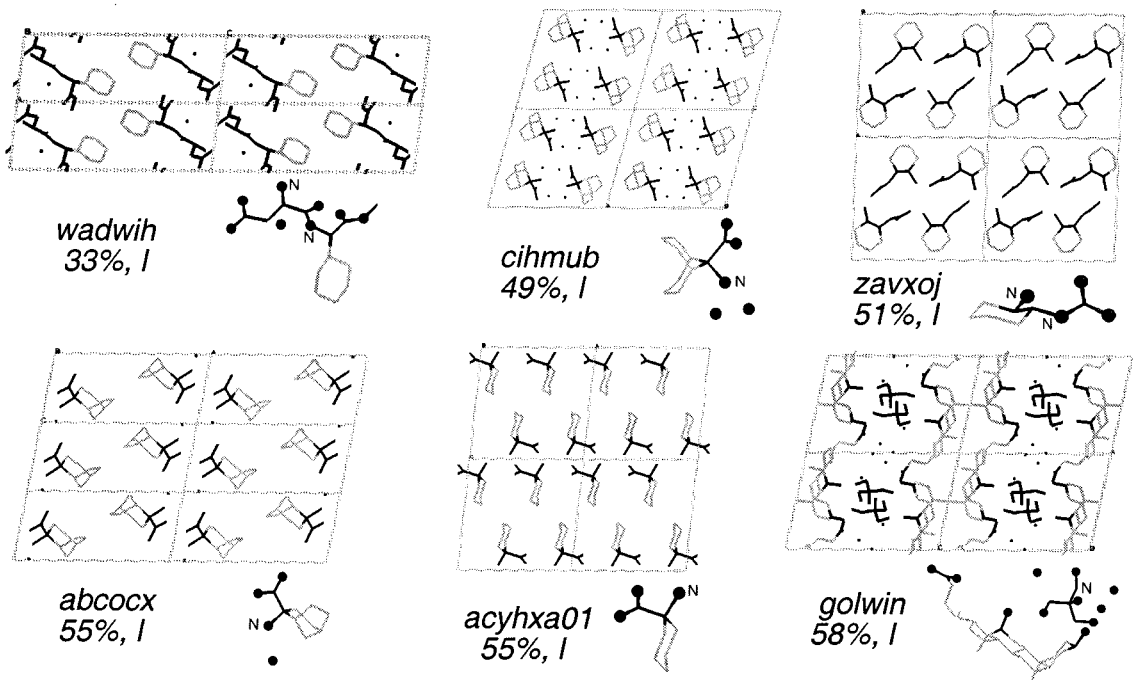

Figure 7. Six lamellar structures from CSD search for cyclohexylammonium carboxylates (see Table 4). Also included are the CSD entry codes, hydrophobic volume fractions, and the molecular structures. Unlabeled spheres are oxygen atoms, vertexes without spheres are carbon atoms. For clarity, hydrogen atoms are omitted. Hydrophobic portion: gray, hydrophilic portion: black.

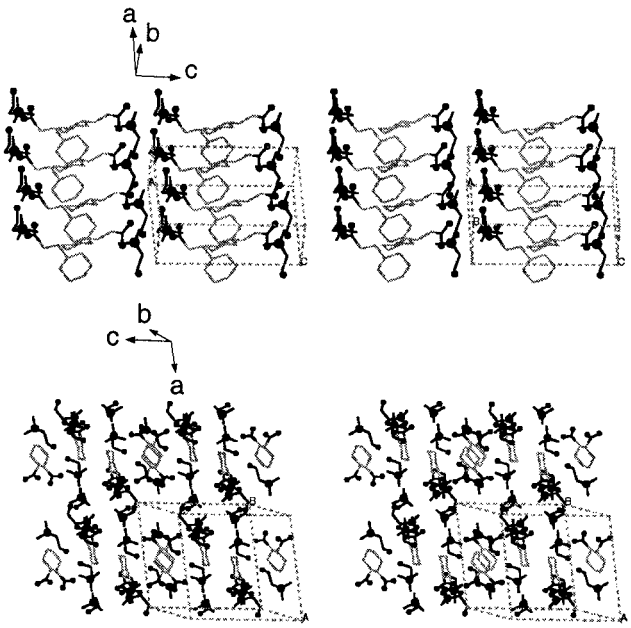

Figure 8. Crystal structures of **3a** (top) and **3c** (bottom). nitrogen atoms: large spheres, oxygen atoms: small spheres; hydrophilic portion: black, hydrophobic portion: gray.

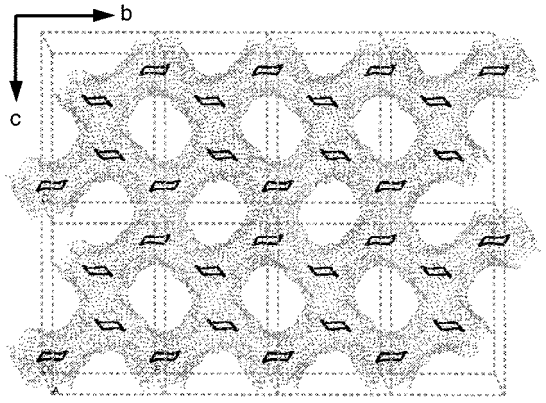

Figure 9. Perforated layer formed by the hydrophobic portion in crystal **3c** and the resultant interfacial surface.[137]

phases are also found, albeit at a smaller probability. Some overlap of structures is therefore expected. The perforated layer is more clearly illustrated in Figure 9. Illustrated in this figure are the hydrophobic aliphatic portions of the crystal. Each aliphatic moiety has three neighboring aliphatic groups in van der Waals contact. The three neighbors are arranged roughly 120° from one another. Such packing generates a honeycomb sheet. The voids in the honeycomb sheet as well as the space between the honeycomb layers are filled by the choline groups. The regular and smooth appearance of the hydrophobic−hydrophilic interface shown in Figure 9 suggests the interface factor is playing an active role in the structure.

The crystal formed in the space group $P2_1/c$ (see Table 2) and the asymmetric unit of the cell consists of one cyclohexanedicarboxylate and two choline groups. The cyclohexanedicarboxylate group adopts the boat conformation, and the carboxylates occupy the equatorial positions. As mentioned earlier, The cyclohexanedicarboxylate groups are organized into distinct layers parallel to the *bc* plane. The overall packing is dense—the van der Waals volume of the molecules takes up 77% of the cell volume. The choline groups are hydrogen-bonded to the carboxylate groups (O−O distances: 2.65, 2.59 Å).

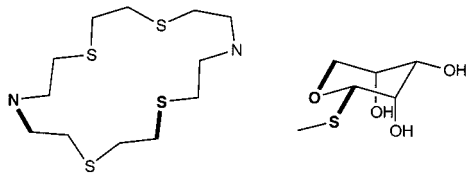

Figure 10. Representative compounds from CSD search for compounds containing thioether and ether groups. (Left) *copjew*; (right) *mtribp10*. Shown in bold are the core units: the C−O bond and the C−S bond.

Ether−Thioethers, Segregation between Hard and Soft. We have thus far examined the interfacial model where the division is between strongly hydrophilic and hydrophobic components. We now wish to see if the interfacial model holds in other two-component systems. We turn to the interfacial division between chemically hard and soft components. As a specific test, we study the system consisting of the relatively soft thioether fragment and the harder ether or amine units. Here we report our findings based on the CSD search and predict the crystal topologies of a few members of this family.

In our CSD search, we looked for thioether compounds containing an ether or amine unit. These core units (thioether, ether, and amine groups) are highlighted in Figure 10. We considered crystals containing only carbon, sulfur, and hydrogen atoms and an additional oxygen or nitrogen atom. We have excluded structures that contain either any multiple bond or any bond between a sulfur atom and an oxygen or nitrogen atom. Also excluded are carbon atoms bonded to none of the following: an oxygen, a nitrogen, or a sulfur atom. This search uncovered 27 crystal structures. Most of them are crown ether or sugar compounds modified by thioether groups, as illustrated in Figure 10.

We divide each crystal structure into the hard and soft portions. Sulfur atoms are soft; nitrogen and oxygen atoms are hard. A carbon atom is considered soft if bonded to sulfur atoms and not to nitrogen or oxygen atoms; it is considered hard if bonded to nitrogen or oxygen and not to sulfur atoms. In the relatively rare case where a carbon atom is simultaneously bonded to sulfur and nitrogen or oxygen atoms, we examined both the case where the carbon atom was considered hard and where it was considered soft.

The structures are classified by the method of closest contacts specified in earlier sections. Again we define the closest contact to be between 1.15 and 1.30 of the van der Waals radii. Within this range, all but one of the 27 structures form into spherical, columnar, perforated lamellar, bicontinuous, and lamellar topologies and the inverse ones. This one exception does not conform to the general structure type for cutoffs between 1.15 and 1.25 as the hard portion forms into both columnar and lamellar domains. At a cutoff of 1.30, however, these discrete domains merge to form a perforated layer structure.

In classifying the structures, we note that the interfacial topologies are more dependent on the cutoff limit of the closest contacts: seven out of the 26 structures change their classifications when one changes the cutoff from 1.15 to 1.30. In particular, three change from the columnar into the bicontinuous type, two from perforated layer to bicontinuous, one from layer to inverse perforated layer, and one switches from inverse sphere to inverse perforated layer. An examination of the 1.15 vs the

Table 6. Structure Types and Hydrophobic-to-Hydrophilic Volume Ratios[a,b] in Ether-thioether Systems

hydrophobic-to-hydrophilic volume ratios (%)	*s*	*c*	*pl*	bi	*l*	*ipl*	*ic*	*is*
10−20	−	1	−	−	−	−	−	−
20−30	2	1	−	−	−	−	−	−
30−40	−	1	1	3	−	−	−	−
40−50	−	−	2	2	1	−	−	−
50−60	−	−	−	1	3	1	−	−
60−70	−	−	−	1	−	−	−	−
70−80	−	−	−	−	−	−	4	1
80−90	−	−	−	−	−	−	−	2

[a] Structural classification is based on closest contacts defined as less than 1.3 times the sum of the van der Waals radii. [b] Carbon atoms simultaneously bonded to sulfur and oxygen atoms are considered soft.

Table 7. Structure Types and Hydrophobic-to-Hydrophilic Volume Ratios[a,b] in Ether-thioether Systems

hydrophobic-to-hydrophilic volume ratios (%)	*s*	*c*	*pl*	bi	*l*	*ipl*	*ic*	*is*
10−20	−	1	−	−	−	−	−	−
20−30	2	1	−	−	−	−	−	−
30−40	−	2	2	1	−	−	−	−
40−50	−	2	2	−	1	−	−	−
50−60	−	−	−	−	3	1	−	−
60−70	−	−	−	1	−	−	−	−
70−80	−	−	−	−	−	−	3	2
80−90	−	−	−	−	−	−	−	1
90−100	−	−	−	−	−	−	−	1

[a] Structural classification is based on closest contacts defined as less than 1.15 times the sum of the van der Waals radii. [b] Carbon atoms simultaneously bonded to sulfur and oxygen atoms are considered soft.

Table 8. Structure Types and Hydrophobic-to-Hydrophilic Volume Ratios[a,b] in Ether−Thioether Systems

hydrophobic-to-hydrophilic volume ratios (%)	*s*	*c*	*pl*	bi	*l*	*ipl*	*ic*	*is*
10−20	1	−	−	−	−	−	−	−
20−30	2	2	−	−	−	−	−	−
30−40	−	2	−	3	−	−	−	−
40−50	−	−	2	3	1	−	−	−
50−60	−	−	−	1	3	1	−	−
60−70	−	−	−	1	−	−	4	−
70−80	−	−	−	−	−	−	−	1
80−90	−	−	−	−	−	−	−	−

[a] Structural classification is based on closest contacts defined as less than 1.3 times the sum of the van der Waals radii. [b] Carbon atoms simultaneously bonded to sulfur and oxygen atoms are considered hard.

1.30 cutoff data shows, however, surprisingly little variation in the overall appearance of the structure type as a function of volume ratios, see Tables 6 and 7. These results suggest, and a detailed examination of the crystal structures supports this suggestion, that there is in fact an almost continuous evolution from columns to perforated layers to bicontinuous or lamellar structures. Changing the cutoff simply shifts the boundaries between these regions.

In Tables 6 and 8 we contrast the two different definitions of hard and soft. In Table 6, carbon atoms simultaneously bonded to sulfur and oxygen or nitrogen atoms are considered soft; in Table 8, such carbon atoms are considered hard. Seven structures contain such carbon atoms. The change in volume ratios can be rather dramatic. For example in *oxttcd*, this change of definition causes the volume ratio to decrease from 91 to 70%. Nevertheless, as a comparison of Tables 6 and 8 shows, the general correlation between structure type and volume ratio is maintained. As one changes the volume ratio, one changes the interfacial boundary. Thus at 91% *oxttcd* is an inverse sphere, while at 70% it is an inverse column.

Overall the interfacial features in the current set resemble the previous ones. As an illustration, we show in Figure 11 the four-layer structures found in this search. As can be seen, in keeping with the interfacial model, the boundary between the hard and soft is generally smooth and regular.

Again, it is possible to predict the crystal topologies for some members of this group. As one can see from the above data, columns and spheres occur at low volume ratio of the soft portion (10−30%), while bicontinuous and lamellar structures form at intermediate region (40−60%). We therefore consider molecules **4a** and **4b**: the soft portion of **4a** accounts for 22%

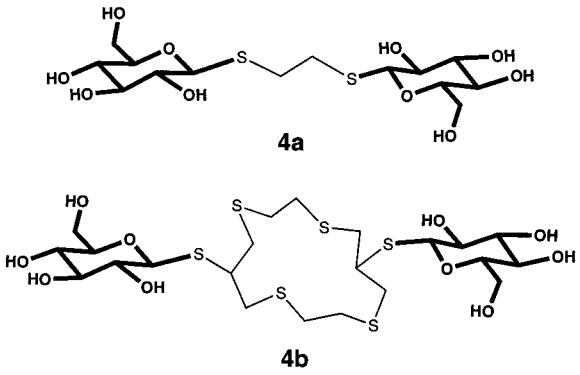

of the total volume, and it is predicted to form in the spherical or columnar topology; the soft portion of **4b** is 52% of the total volume and is predicted to form in the lamellar or bicontinuous structure type.

Aromatic Oxo−Metal Complexes. In our final CSD search we considered structures containing a benzenoid ring, an ethylene oxide fragment, and a bond between a metal and an oxygen atom. These core units are illustrated in Figure 12. We considered structures containing only carbon, oxygen, hydrogen, and metal ions. In addition, we excluded structures containing aliphatic carbon atoms not bonded to oxygen atoms.

This search was therefore quite different from our earlier searches. For, while in previous CSD studies we considered molecules decomposable into two and only two chemical components, here it is possible to have three chemically distinct regions: to wit, the region of ionic metal atoms, the hydrophilic region filled with oxygen atoms bound to carbon but not to the metal, and the hydrophobic aromatic portion of the molecule. Thus, as we shall see, the proper block copolymer analogue for these phases need not be diblock copolymers but rather the triblock copolymers.

This search uncovered 51 structures, most of which are aromatic crown ethers or caboxylic acid molecules coordinated to metal ions. As a first attempt to analyze these structures, we divided the crystal structures into just two regions: the hydrophobic region consisting of the ethylene oxide and the metal−oxo groups and the hydrophobic region derived solely from the aromatic rings. The topology of the interface between these two portions is determined by the method of closest contacts outlined in earlier sections.

Shown in Tables 9 and 10 are the structural breakdowns with the closest contact respectively defined as 1.15 and 1.30 times the van der Waals radii. In the former case, 50 of the 51 structures belong to the five general structural topologies:

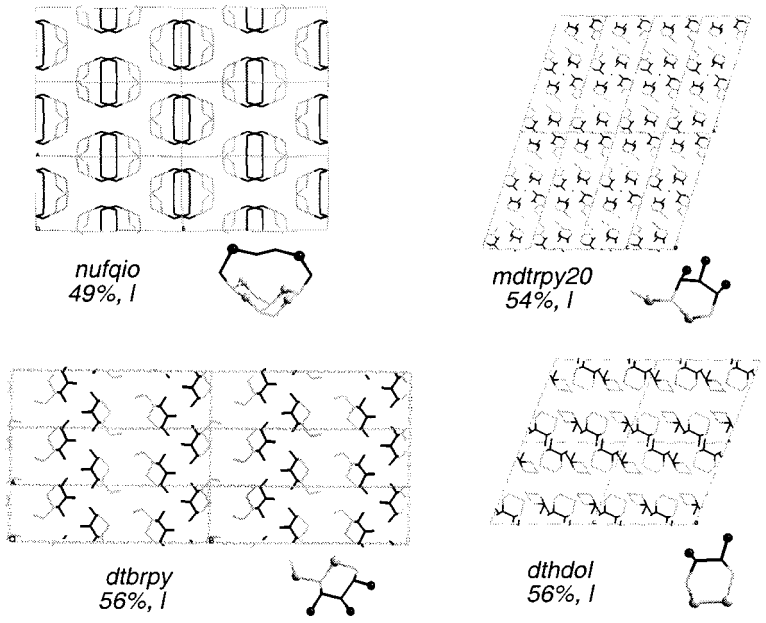

Figure 11. Four lamellar structures of Table 6 for thioether−ether compounds. Also included are the CSD entry codes, soft volume fractions, and the molecular structures. Soft portion: gray, hard portion: black. Gray spheres: sulfur atoms, black spheres: oxygen atoms.

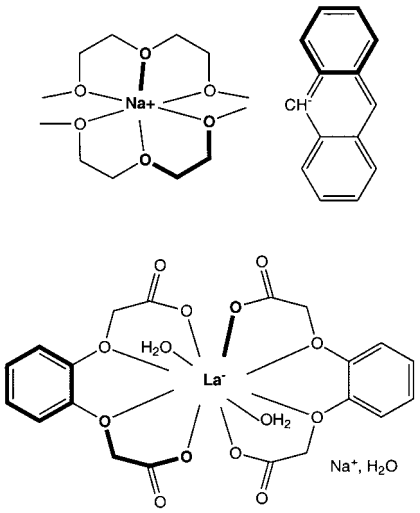

Figure 12. Representative compounds from CSD search for aromatic ammonium carboxylates. Top: *wipxey*, bottom: *abxala*. Shown in bold are the core units: the benzenoid ring, the ethylene oxide unit, and the oxygen metal bond.

Table 9. Structure Types and Hydrophobic-to-Hydrophilic Volume Ratios[a] in Aromatic Oxometal Complexes

hydrophobic-to-hydrophilic volume ratios (%)	*s*	*c*	*pl*	bi	*l*	*ipl*	*ic*	*is*
10−20	–	–	–	–	–	–	–	–
20−30	1	2	3	–	3	–	–	–
30−40	–	–	7	3	4	–	–	–
40−50	–	–	4	9	1	–	–	–
50−60	–	–	–	3	2	4	–	–
60−70	–	–	–	–	–	–	1	2
70−80	–	–	–	–	–	–	–	2
80−90	–	–	–	–	–	–	–	–

[a] Structural classification is based on closest contacts defined as less than 1.30 times the sum of the van der Waals radii.

spheres, columns, perforated layers, bicontinuous structures, and layers. In the latter case all 51 can be so classified. These five crystal topologies are clearly energetically preferred.

Table 10. Structure Types and Hydrophobic-to-Hydrophilic Volume Ratios[a] in Aromatic Oxometal Complexes

hydrophobic-to-hydrophilic volume ratios (%)	*s*	*c*	*pl*	bi	*l*	*ipl*	*ic*	*is*
10−20	–	–	–	–	–	–	–	–
20−30	1	4	1	–	3	–	–	–
30−40	–	1	8	1	4	–	–	–
40−50	1	2	2	5	1	–	–	–
50−60	–	–	–	4	2	5	–	–
60−70	–	–	–	–	–	–	1	2
70−80	–	–	–	–	–	–	–	2
80−90	–	–	–	–	–	–	–	–

[a] Structural classification is based on closest contacts defined as less than 1.15 times the sum of the van der Waals radii.

As one shifts the cutoff distance of closest contact from 1.15 to 1.30 times the van der Waals radii, nine out of the 51 structures change classifications. As can be seen from Tables 9 and 10, the general shift in increasing the cutoff distance is that columnar phases become perforated layer topologies and perforated layer phases turn into bicontinuous structures.

Overall, the relation between structure types and volume ratios is somewhat maintained. It may be seen, however, that there are a number of differences between the results given in Tables 9 and 10 and those discussed earlier. First, while in the earlier CSD searches there were three times more columnar structures than perforated layer structures (28 to 8), here we see many more perforated layer structures. For example, at a closest contact defined as 1.3 times the van der Waals radii, there are 12 perforated layer structures and only two columnar structures.

Perhaps even more interesting are the layer structures. In Figure 13 we show seven of the 10 layer structures reported in Table 9 (the others are given in the Supporting Information). The following convention is used. The aromatic region is shown in green, the metal, the oxygen atoms coordinated to it, and the included water molecule are shown in red, and the oxygen atoms not bonded to the metal atom together with the aliphatic carbon atoms are shown in brown. In *zegpeg*, the structures with volume ratios of 25%, the lowest of the entire group, one sees clearly

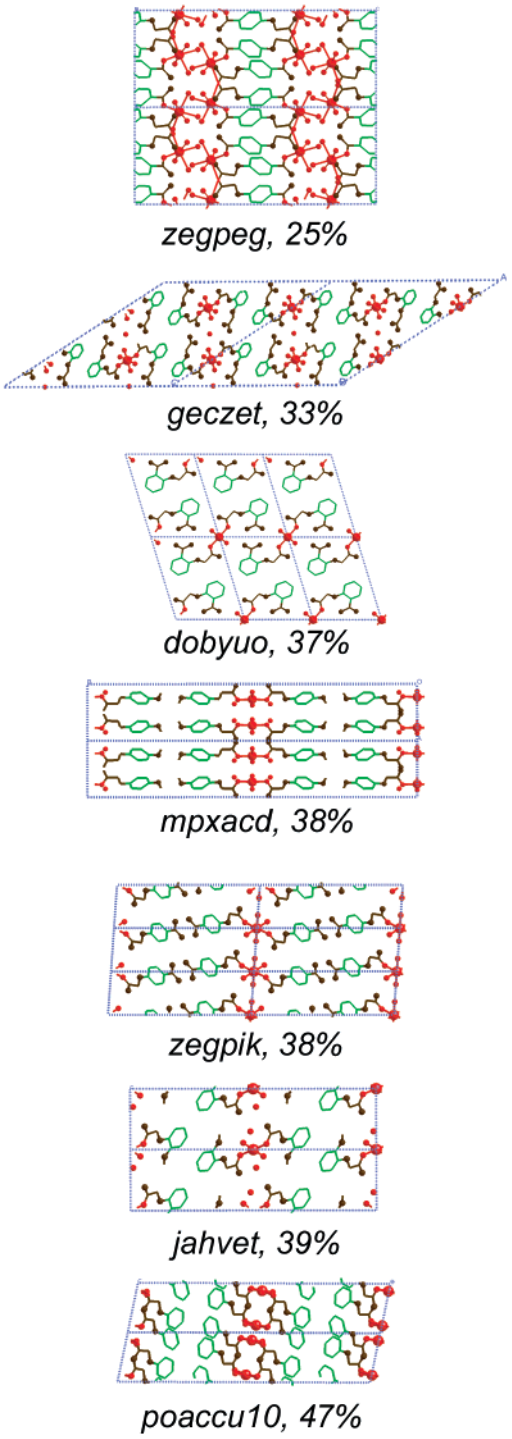

Figure 13. Seven lamellar structures from the CSD search of aromatic oxo-metal complexes. Ionic portion: red, hydrophilic portion: brown, aromatic portion: green. Large sphere: metal ion, small sphere: oxygen atom. For clarity, hydrogen atoms are omitted.

the layer topology. However, this is not a layer topology composed of just two fractions. Rather, the ionic portion (red), the hydrophilic portion (brown), and the hydrophobic portion shown (green) each form a separate layer. This same separation into three layer types is clear in other lamellar phases as well. It is most clear in *mpxacd*, *geczet*, *zegpik*, *jahvet*, and *poaccu10*, as is shown in Figure 13.

Here we see concrete evidence that a three-component analysis is more appropriate than the two-component analysis

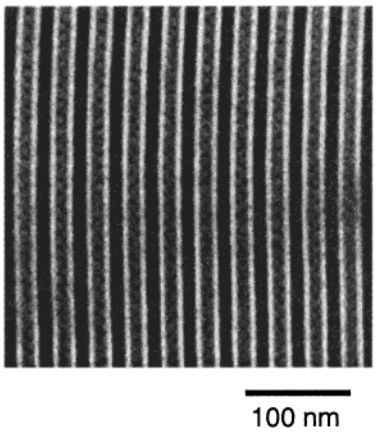

Figure 14. Transmission electron micrograph of the lamellar phase in the isoprene(I)−styrene(S)−2-vinylpyridine(P) triblock copolymers. The black, white, and gray images correspond to the I, S, and P domains, respectively.[133]

in the previous sections. We therefore turn to the triblock topologies as opposed to diblock topologies. There has recently been much work on triblock copolymers.[133,138−140] It has been found that triblock systems form in much more complex topologies than diblock systems. For example, columnar structures are known to further subdivide into at least six separable columnar topologies. However, certain principal features of triblock copolymers are well-established. One of the principal triblock topologies is the ABC lamellar structure in which the three different components separate in layers one from another. One such ABC lamellar structure is shown in Figure 14. The similarity between this structure and the trilayer systems in Figure 13 is clear. It is possible that the remaining structures in Tables 9 and 10 correspond to some other triblock topologies. There are, however, so many triblock topologies and the field is still so comparatively new that it is a rather daunting task to correlate the structures in Table 7 more fully with such triblock structure types.

Conclusions

In the preceding section we considered four different types of two-component crystals: aromatic ammonium carboxylates, aromatic oligo(ethylene oxides), cyclohexylammonium carboxylates, and ether−thioethers. In each of these four classes our CSD study showed that five crystalline topologies are dominant: spheres, columns, perforated layers, layers, and bicontinuous structures. Of the 111 structures examined, 108 belonged to one of these five types, see Table 11. A key predictor for the crystalline topology is the volume fraction of one chosen component. As shown in Table 11, for volume fractions of 20−30% four-fifths are of spherical or columnar type, and for fractions of 40−50% four-fifths have lamellar or bicontinuous topologies.

We have shown that this analysis can be used to predict crystalline topologies. On the basis of the volume ratios of the two components, we have predicted that three molecules should

(137) This is the dot display of the Connolly surface of the hydrophobic fragments. It is generated by rolling a spherical probe of a specific radius (1.4 Å) over the van der Waals surface of the hydrophobic fragments.
(138) Bates, F. S.; Fredrickson, G. H. *Phys. Today* **1999**, *52*, 32.
(139) Matsen, M. W. *J. Chem. Phys.* **1998**, *108*, 785.
(140) Stadler, R.; Auschra, C.; Beckmann, J.; Krappe, U.; Voigt-Martin, I.; Leibler, L. *Macromolecules* **1995**, *28*, 3080.

Table 11. Overall Correlation between Structure Types and Hydrophobic-to-Total Volume Ratios

volume ratios (%)	*s* and *c*	*pl*	*bi* and *l*	*ipl*	*ic* and *is*
0−10	1	−	−	−	−
10−20	2	−	−	−	−
20−30	18	1	4	−	−
30−40	11	5	13	−	−
40−50	−	4	18	−	−
50−60	−	−	13	5	1
60−70	−	−	1	2	0
70−80	−	−	−	−	6
80−90	−	−	−	−	3

[a] Structural classification is based on closest contacts defined as less than 1.30 times the sum of the van der Waals radii.

adopt a columnar topology and that another three should adopt a layer or bicontinuous structure. Five of these six predictions were borne out by subsequent experimental work. One of the predicted columnar structures, however, proved to be of perforated layer type.

The approach adopted in this paper, that of concentrating on the interface between the two components in the crystal, seems a valid guide to the rationalization and prediction of crystalline topologies. It also appears to be reasonably general: it can be applied equally well to ether−thioethers, aromatic olio(ethylene oxides), and cyclohexylammonium carboxylates.

However several caveats needs to be recalled. First, as in the case of aromatic oxo−metal complexes, the system in question must be a two-component and not a three-component system. Three-component systems have much more complex structural topologies than diblock systems. Second, there must be no local interaction which enforces a certain type of global architecture independent of the two-component volume ratio. One well-known example of such overriding local interactions is the interdigitation of the parallel alkyl chains.[141,142] Such alkyl chains pack into layers and impose the lamellar topology on the resultant crystal structure, irrespective of the two-component volume ratio.

The approach described in this paper can be considered a top-down approach. We concentrated on a global feature of the crystal structure, that is, the two-component interface, and then sought to find molecules which comfortably fit within this interface. But such a top-down approach could, in principle, be most effective when coupled with a complementary bottom-up approach, that is, an analysis where one concentrates first on local interactions and then envisions how such local interactions can affect the global crystal structure.

An example of such a combined approach can be found in the porous organic crystal literature.[27,46,72,113,143] In this work, the synthetic target is generally a hexagonal or pseudohexagonal structure in which the crystal forms a honeycomb matrix and the solvent lies in the interior hexagonal columns. This architecture is therefore the columnar architecture discussed in this paper, where the major component is the crystalline framework and the minor component is the solvent. While such an architecture is a natural one, its formation is abetted by the choice of molecular building blocks which are predisposed to form honeycomb channels.[129]

It is also possible to unite top-down and bottom-up approaches by joining the ideas of this paper with those of Kitaigorodsky.[144] For example, Kitaigorodsky has enumerated the ways by which molecules can pack to form columns. Most commonly the molecular fragments of the column are related by one of the crystallographic symmetry elements, namely, the two-fold screw, the inversion center, the glide plane, or the translational operation. Among the two dozen or so columnar structures studied in this paper, 14 of the individual columns are based on the two-fold screw, six are based on inversion center, and four on glide planes, while the remaining six consist of basic translational units containing only one molecular fragment. One can thus envision that one could first use the volume ratio to determine the basic interface type and then use local atom−atom potentials or ab initio quantum theory, together with these simple symmetry operations, to accurately predict full crystal structures.

Acknowledgment. This work was supported by the National Science Foundation (Grant DMR-9812351). We thank Mr. Abhijit B. Mallik for assistance in preparing the organic compounds. We also thank Mr. Nathan Emmott for assisting in the calculation of volume ratios.

Supporting Information Available: Figures of the molecules from CSD search and their corresponding crystal structures; tables of crystal refinement data, bond distances, bond angles, anisotropic thermal factors for compounds **1a**, **1c**, **2c**, **3a** and **3c**; experimental and calculated powder diffraction data for the above compounds (PDF). This material is available free of charge via the Internet at http://pubs.acs.org.

JA0115518

(141) Abrahamsson, S.; Lundén, B. M. *Acta Crystallogr., Sect. B* **1972**, *28*, 2562.
(142) Taga, T.; Miyasaka, T. *Acta Crystallogr., Sect. C* **1987**, *43*, 748.
(143) Kiang, Y.-H.; Gardner, G. B.; Lee, S.; Xu, Z. *J. Am. Chem. Soc.* **2000**, *122*, 6871.
(144) Kitaigorodsky, A. I. *Molecular crystals and molecules;* Academic Press: New York, 1973; pp 21−37.